

Available at www.sciencedirect.comjournal homepage: www.elsevier.com/locate/ijhydene

Model-based determination of hydrogen system emissions of motor vehicles using climate-chamber test facilities

Martin Weilenmann^{a,*}, Christian Bach^a, Philippe Novak^a, Andrea Fischer^b, Matthias Hill^b

^aEMPA, Swiss Federal Laboratories for Materials Testing and Research, I.C. Engines Laboratory, CH-8600 Duebendorf, Switzerland

^bEMPA, Swiss Federal Laboratories for Materials Testing and Research, Air Pollution/Environmental Technology Laboratory, CH-8600 Duebendorf, Switzerland

ARTICLE INFO

Article history:

Received 21 March 2007

Received in revised form

28 September 2007

Accepted 28 September 2007

Available online 26 November 2007

Keywords:

Fuel cell

Gaseous fuels

Hydrogen

System emissions

Test cell

Concentration measurement

ABSTRACT

Because of air quality problems, the problem of CO₂ related greenhouse gas emissions and shortage of fossil fuels, many vehicles with gaseous fuels (CNG, biogas, hydrogen, etc.) are under research and development. Such vehicles have to prove that both their exhaust emissions and their overall system emissions (including running loss) remain below certain safety limits before they can be used in practice. This paper presents a cost-effective way of monitoring such system emissions from hydrogen or other gaseous fuel powered vehicles within an air-conditioned chassis dynamometer test cell, as commonly used for low ambient emission tests on gasoline vehicles. The only additional equipment needed is a low-concentration sensor for the gas of interest (e.g. hydrogen). The method is based on concentration measurements and a dynamic mass balance model. It is shown by a real experiment that very low emissions can be recorded. Additionally, error bounds and sensitivities on different parameters such as air exchange ratio are quantified.

© 2007 International Association for Hydrogen Energy. Published by Elsevier Ltd. All rights reserved.

1. Introduction

Vehicles with gaseous fuels are becoming more and more common as they show many advantages compared to gasoline or diesel fuelled cars [1]. In some countries LPG is significantly cheaper than liquid fuels since it is left behind as “waste” in the refinery process. Natural gas as fuel offers notable CO₂ and exhaust emission benefits over gasoline and diesel. In addition, the production of biogenic methane that can be used as natural gas shows one of the highest field-to-wheel efficiencies and the best CO₂ balance among biofuels and additionally can be produced from waste [1]. Hydrogen as fuel for fuel cells as well as for I.C. engines is likely to play an important role in future vehicle propulsion technology. The development of hydrogen-powered vehicles is also driven by

air quality factors, the problem of CO₂ and other greenhouse gases and fossil fuel supply dependency [2,3].

For all these gaseous fuels there are different fuel storage systems such as high-pressure gas bottles, low temperature liquidation, metal hydrides and others, operating at a certain overpressure. Thus, it is of great interest to developers, manufacturers and legislators to be able to monitor the overall system emissions of these gaseous fuels under realistic conditions. This holds for both the case of a parked car subject to changing ambient conditions and emissions at system start, while running and at system stop [4,5].

All these situations can be simulated on chassis dynamometers embedded in climatic chambers. However, it is only possible with enormous effort to keep such climatic chambers so airtight that the evaporative emissions can be

*Corresponding author. Tel.: +41 44 823 46 79; fax: +41 44 823 40 44.

E-mail address: martin.weilenmann@empa.ch (M. Weilenmann).

measured by monitoring the increasing gas concentration within the chamber directly. The methods to monitor evaporative hydrocarbon emissions from gasoline vehicles described in [6,7] allow either the measurement in an airtight chamber (SHED = sealed housing for evaporative determination) or the measurement with the so-called point source method. While the SHED-method works well for test on the standing car, severe sealing problems occurred for running-loss tests, where a chassis dynamometer is needed within the SHED. For hydrogen in particular, the sealing of the housing poses even more of a challenge than for evaporative emission measurement of hydrocarbons. In the alternative point source method all potential points of leakage as fuel tank cap or vent opening need to be equipped with funnels leading to an analyser with an appropriate air flow, strong enough to collect all emissions but small enough to keep concentrations measurable. Thus, this method results in rather extended equipment that needs to be adapted to each vehicle, and one cannot be sure that the total of evaporative emissions is really monitored.

Alternatively this paper presents a method to monitor running loss and system emissions of gas-fuelled cars by applying the mass balance method to a climatic test cell with ventilation. It is shown what sensor equipment is needed and how the source emissions are calculated. The method is validated by tests. A sensitivity analysis is also presented showing what limiting conditions have to be fulfilled to reach a certain quality of measurement.

2. Methodology

2.1. Mass balance

The basic idea of this approach is the fact that atoms cannot vanish. Based on Fig. 1 showing a chassis dynamometer in a climatic chamber, this leads to the mass balance of Eq. (1). The change in mass of a gaseous matter (subsequently called gas G) inside the chamber is the difference between all mass flowing into the chamber and all mass flowing out of the chamber. This assumes that no chemical reactions between the gas concerned and other matter take place. This is typically true of hydrogen, methane or propane at ambient conditions and concentrations below 1 ppm [8].

$$\frac{\partial m_G}{\partial t} = \sum \dot{m}_{G,in}^* - \sum \dot{m}_{G,out}^*$$

$$\frac{\partial m_G}{\partial t} = \dot{m}_{G,vent,in}^* + \dot{m}_{G,car}^* - \sum \dot{m}_{G,out}^* \quad (1)$$

$\frac{\partial m_G}{\partial t}$ denotes the change in mass of gas G within the cell, $\sum \dot{m}_{G,in}^*$ the sum of all mass flows of gas G into the chamber and $\sum \dot{m}_{G,out}^*$ the sum of all mass flows of gas G out of the chamber, $\dot{m}_{G,vent,in}^*$ the mass flow into the chamber from ventilation and $\dot{m}_{G,car}^*$ the source flow of interest. All variables are functions of time.

A mass flow of gas G into the chamber occurs if this matter is found in the ambient air. Thus, the mass flow of ventilation air and the concentration of gas G in the intake air need to be

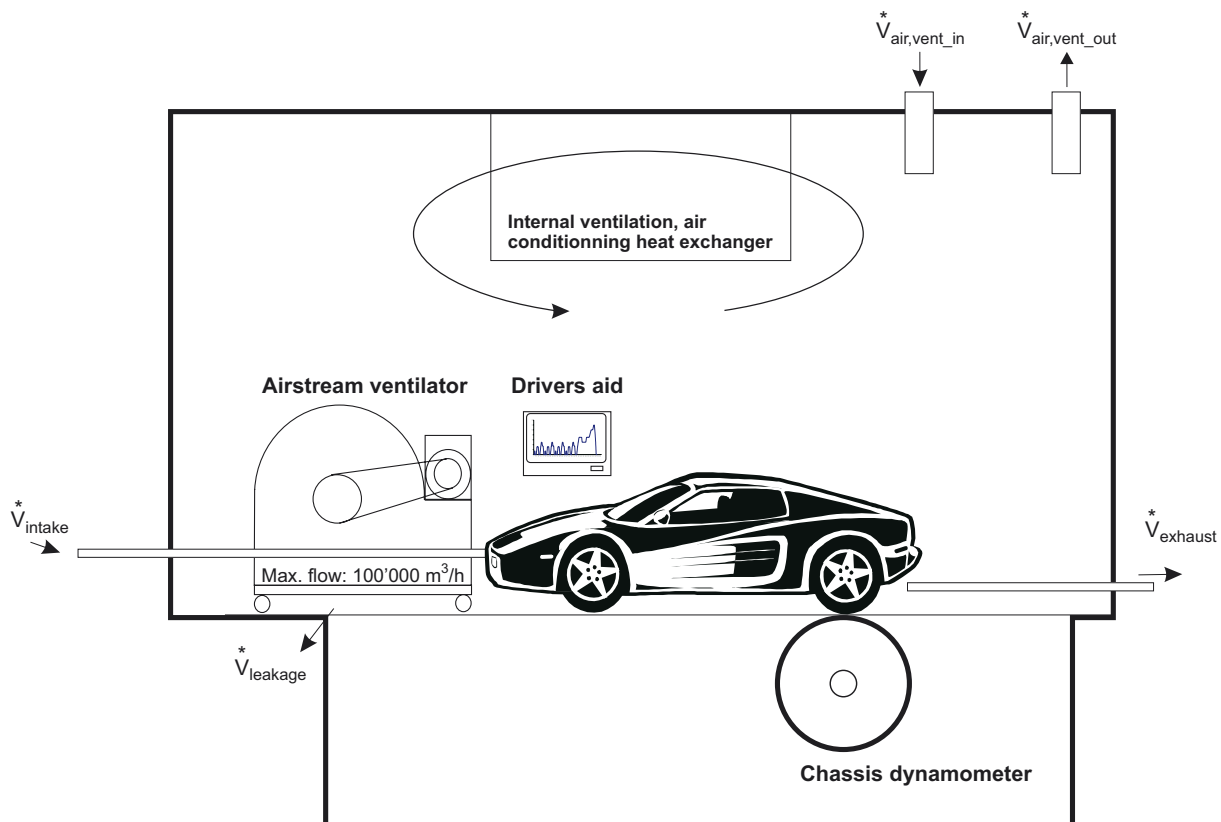


Fig. 1 – Sketch of climatic chamber with ventilation flows.

measured. The second mass flow into the chamber is the evaporation from the vehicle, which is of interest.

There are different possibilities for flows of gas G out of the chamber:

- Intended ventilation.
- *Leakage*. The doors of the chamber as well as channels for cables and pipes are not airtight, so some air leaks. Most climatic chambers operate with a slight overpressure to ensure that air flows out at all openings, since inflowing humid air, when operating at low temperatures, would cause dangerous ice formation and additionally disturb the humidity control of the chamber (Fig. 1).
- If the vehicle is running and is propelled by a system that consumes air (engine or fuel cell system), either the corresponding air supply can be from outside the chamber or air from the room is used. Since the exhaust gases are typically led outside the chamber and measured there, the latter case is also an outflow for the mass balance of gas G.

It is obviously not possible to measure the mass flow and concentrations of gas G at all the outflow locations, but this problem can be bypassed by the following approach.

The chassis dynamometers for exhaust emission measurements are equipped with fans for the cooling of the vehicle. Together with the ventilation of the air conditioning of the cell, this can cause such high turbulence that the concentration of gas G in the room can be considered to be homogeneously distributed. In other words the mixing time constant in the room must be significantly lower than the air exchange rate. It must be ensured that no dead zones where ventilation is poor exist inside the climatic chamber. In other words, in most cases where chassis dynamometers are installed in climatic cells, the rolls of the dynamometer as well as the breaking electric motor are in an under-floor compartment that is contained in the cell. It must therefore be possible for this compartment to be ventilated intentionally by opening covers and adding additional ventilators.

If the concentration of gas G inside the chamber is indeed homogenous and measured, this concentration also holds for all the outflows of the cell. As long as the pressure remains stable within the cell, which is controlled by the ventilation, the total mass flow of air out of the cell is equal to the flow into the cell. It is thus sufficient to measure the air inflow.

In addition, since the concentration inside the climatic chamber is homogenous, it needs to be measured at just one location.

Naturally, a flow of gas G as the inflow $\dot{m}_{G,vent,in}^*$ cannot be measured directly. By assuming ideal gases, it may be determined as follows. Any mass flow of air \dot{m}_{air}^* is the product of air density ρ_{air} and volume flow \dot{V}_{air}^* .

$$\dot{m}_{air}^* = \rho_{air} \dot{V}_{air}^* \quad (2)$$

The contained mass flow of gas G then is

$$\dot{m}_G = c_G \rho_G \dot{V}_{air}^* \quad (3)$$

where c_G is the concentration of gas G and ρ_G its density. Since the tests take place in a climatic chamber and do not last for days, it may be assumed that both temperature and pressure

remain stable, and thus that densities are constant. It is thus sufficient to measure the volume flow of air and the concentration of gas G to determine its mass flow. For the chamber it correspondingly holds that

$$\dot{m}_G = c_G \rho_G \dot{V}_{ch} \quad (4)$$

The index ch stands for chamber. Assuming that the volume flow of air out of the chamber is equal to the inflow and that the distribution of gas G in the chamber is homogenous, Eqs. (1)–(4) give

$$\frac{\partial c_{G,ch}}{\partial t} \rho_G \dot{V}_{ch} = c_{G,vent,in} \rho_G \dot{V}_{air,vent,in}^* + \dot{m}_{G,car}^* - c_{G,ch} \rho_G \dot{V}_{air,vent,in}^* \quad (5)$$

And this can be solved for the mass flow of the source, thus the car

$$\dot{m}_{G,car}^* = \frac{\partial c_{G,ch}}{\partial t} \rho_G \dot{V}_{ch} - c_{G,vent,in} \rho_G \dot{V}_{air,vent,in}^* + c_{G,ch} \rho_G \dot{V}_{air,vent,in}^* \quad (6)$$

So, the system emissions as mass per time unit can be calculated by knowing the chamber volume, the density of gas G (thus temperature and pressure) and measuring the volume flow of air into the chamber as well as the gas concentration of G inside the chamber and in the air intake. As pressure and temperature in inflow and outflow are alike, densities for both flows can be considered to be equal.

2.2. Measurement equipment

A commercial gas chromatograph (Reduction Gas Analyzer (RGA3), Trace Analytical Inc., California, USA) was used to measure H₂ inside the climatic chamber. The RGA3 is an ultra-trace level gas detection system capable of monitoring low ppb concentrations of reducing gases such as H₂. The instrument consists of a microprocessor-controlled gas chromatograph which utilises method of reduction gas detection.

Synthetic air preconditioned by molecular sieve 5 Å and SOFNOCAT to remove H₂O and reaction impurities (CO and H₂) is used as carrier gas. Aliquots of air samples are flushed with a rate of 20 ml/min over a 1 ml sample loop. After equilibration, the sample volume is injected onto the columns. Sample components of interest are separated chromatographically in an isothermal mandrel-heating column oven. The chromatographic precolumn (Unibeads 1S, 60/80 mesh; 1/8" × 30") is mainly used to remove CO₂, H₂O and hydrocarbons. Subsequently H₂ and CO are separated by the analytical column (molecular sieve 5 Å, 60/80 mesh; 1/8" × 30") and pass into the detector which contains a heated bed of mercuric oxide. Within the bed a reaction between mercuric oxide (solid) and H₂ occurs and the resultant mercury vapour in the reaction is quantitatively determined by means of an ultraviolet photometer located immediately downstream of the reaction bed. The columns are kept at 75 °C; the detector is heated to 270 °C. The amount of H₂ in the air sample is proportional to the amount of mercury that is determined.

During the quasi-continuous observations of the H₂ concentration in the test chamber, measurements were taken

every 2 min. At the beginning and end of each test cycle the ambient air concentration (concentration of the ventilation inflow) was measured for 30 min. Typically the concentrations were very constant over the short time of one test cycle and in the range of the mean of 576 ± 94 ppb at Duebendorf [9].

Two high concentration reference gases (50 and 100.2 ppm H_2 ; Messer Schweiz, Switzerland) were dynamically diluted with zero air to the range of interest by means of a dilution unit (MKAL diluter, Breitfuss Messtechnik GmbH, Harpstedt, Germany). The dilution unit was indirectly referenced against the primary gas flow standard of the Swiss Federal Office of Metrology. The different mixtures of the two high concentration standards showed excellent agreement with each other and the NOAA/GDM scale [10]. Detection limit for H_2 was ± 10 ppb and the standard uncertainty of the measurement 5%.

2.3. Analysis methodology

As described in the previous section the low concentrations of the gases of interest cannot be measured with high time resolution, i.e. within seconds. The equipment described above allows a sampling rate of 2 min. Thus Eq. (6) needs to be solved discretely.

The most direct and simple approach of discretisation is replacing the derivative of the chamber concentration by the difference of the last two measured values. For time step k this results in

$$\frac{\partial c_{G, \text{ch}}}{\partial t}(t = kT) \approx \frac{c_{G, \text{ch}, k} - c_{G, \text{ch}, k-1}}{T}, \quad (7)$$

where T is the sampling interval [11]. Since both ambient concentration of gas G and ventilation air flow typically change very little over one time interval, it does not matter if the values at the beginning or the end of the sampling interval are used. The chamber concentration, however, may change substantially; thus average concentration during one sampling step is approximated by the mean of the values measured at either end of it. The mass balance results in

$$\begin{aligned} \dot{m}_{G, \text{car}, k}^* &= \frac{c_{G, \text{ch}, k} - c_{G, \text{ch}, k-1}}{T} \rho_G V_{\text{ch}} - c_{G, \text{vent}, \text{in}, k} \rho_G \dot{V}_{\text{air}, \text{vent}, \text{in}, k}^* \\ &+ \frac{c_{G, \text{ch}, k} + c_{G, \text{ch}, k-1}}{2} \rho_G \dot{V}_{\text{air}, \text{vent}, \text{in}, k}^*. \end{aligned} \quad (8)$$

So the mass emitted during the sampling interval k is

$$\begin{aligned} m_{G, \text{car}, k} &= \rho_G \left((c_{G, \text{ch}, k} - c_{G, \text{ch}, k-1}) V_{\text{ch}} + \dot{V}_{\text{air}, \text{vent}, \text{in}, k}^* T \right. \\ &\quad \left. \times \left(\frac{c_{G, \text{ch}, k} + c_{G, \text{ch}, k-1}}{2} - c_{G, \text{vent}, \text{in}, k} \right) \right). \end{aligned} \quad (9)$$

Mathematically more complex but also more accurate is the discretisation by solving the differential equation (5) analytically for one time step, what needs certain assumptions.

Here there is freedom to assume all input signals (i.e. $\dot{V}_{\text{air}, \text{vent}, \text{in}}^*(t)$, $c_{G, \text{vent}, \text{in}}(t)$, $\dot{m}_{G, \text{car}}^*(t)$) as arbitrary functions of time. Hence, if necessary it might be possible to measure the ventilation air flow at high time resolution and use that time function for the calculus, but usually this flow is reasonably constant. The ambient concentration of the gas G typically is constant too if not working downwind of a huge non-uniform gas source. Of course the time function $\dot{m}_{G, \text{car}}^*(t)$ of how the vehicle emits the gas G is unknown. If the total mass emitted during one time step $m_{G, \text{car}, k}$ is given, the most extreme case for the calculus is if all of it is released immediately after the time interval starts or immediately before the time interval ends (peak functions, Fig. 2). The “average” case happens if the vehicle is constantly emitting gas G . For benchmarking the quality of this methodology in Section 3.2, Eq. (5) is solved subsequently for all three assumptions.

In the case of the early peak, the solution of Eq. (5) for the time $t = kT$ is

$$c_{G, \text{ch}, k} = c_{G, \text{vent}, \text{in}} + \left(c_{G, \text{ch}, k-1} + \frac{m_{G, \text{car}}}{\rho V} - c_{G, \text{vent}, \text{in}} \right) e^{-(\dot{V}/V)T}, \quad (10)$$

and thus, the mass of gas G emitted in one time period is

$$m_{G, \text{car}, k} = \rho V \left(\frac{c_{G, \text{ch}, k} - c_{G, \text{vent}, \text{in}}}{e^{-(\dot{V}/V)T}} + c_{G, \text{vent}, \text{in}} - c_{G, \text{ch}, k-1} \right). \quad (11)$$

For the late peak case we obtain

$$c_{G, \text{ch}, k} = c_{G, \text{vent}, \text{in}} + (c_{G, \text{ch}, k-1} - c_{G, \text{vent}, \text{in}}) e^{-(\dot{V}/V)T} + \frac{m_{G, \text{car}}}{\rho V}, \quad (12)$$

$$m_{G, \text{car}, k} = \rho V (c_{G, \text{ch}, k} - c_{G, \text{vent}, \text{in}} + (c_{G, \text{vent}, \text{in}} - c_{G, \text{ch}, k-1}) e^{-(\dot{V}/V)T}). \quad (13)$$

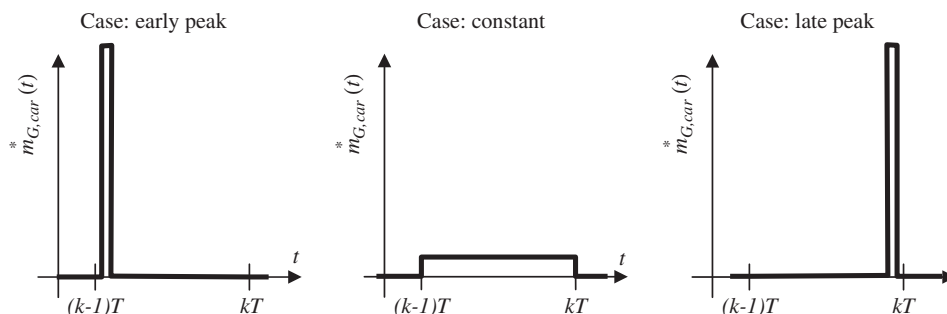


Fig. 2 – Most extreme possibilities of time functions of gas release for benchmarking.

And for the average case of a constant emitting source $\dot{m}_{G,car}(t) = m_{G,car,k}^*/T$:

$$c_{G,ch,k} = c_{G,vent_in} + \frac{m_{G,car}^*}{\rho T \dot{V}} + \left(c_{G,ch,k-1} - c_{G,vent_in} - \frac{m_{G,car}^*}{\rho T \dot{V}} \right) e^{-(\dot{V}^*/V)T}, \quad (14)$$

$$m_{G,car,k}^* = \frac{\rho T \dot{V}^*}{V} \left(\frac{c_{G,ch,k} - c_{G,ch,k-1} e^{-(\dot{V}^*/V)T}}{1 - e^{-(\dot{V}^*/V)T}} - c_{G,vent_in} \right). \quad (15)$$

Even though Eqs. (11), (13) and (15) look rather different, their outputs remain similar as long as the sampling interval T is small compared to the ventilations time constant V/\dot{V} . So the quality of this method rises if both the sampling interval and ventilation are small. Realistic examples are given in the next section, where both the different methods (Eqs.(11), (13) and (15)) and different sampling intervals are applied to the same test data to highlight how accuracy depends on the different parameters of the system.

3. Example and sensitivity analysis

The test examples described here were conducted in the climatic cell chassis dynamometer of Empa. All numeric values belong to this test equipment.

3.1. Determination of chamber volume

Estimating the air volume in the chamber by geometrical means is quite difficult, since the volumes of car, ventilators, heat exchange units, etc., are difficult to describe. Thus a test where a well-defined volume of helium was released immediately and its concentration was measured subsequently, while external ventilation was closed but internal circulation was on, allowed the chamber volume to be estimated from the dilution ratio. The value was found to be 256 m^3 with a standard deviation of 8 m^3 .

3.2. Identification of volume flow and validation

If the volume flow of the ventilation is not possible to be measured directly, but is constant over time, it is possible to determine it by the following test.

As above, a certain volume of a measurable gas such as helium is injected into the cell (with ventilation running). After the mixing phase in the cell the helium concentration will follow Eq. (5) or one of its solutions (10), (12) or (14) with a zero source activity of the car $\dot{m}_{G,car}(t) = 0$. Measurements are shown in Fig. 3. Subtracting the background concentration and building the logarithm of the He concentration result in a straight line for the first 2000s where concentrations are reasonably above the detection limit.

The gradient of this straight line is directly the air exchange rate, thus \dot{V}/V . Its inverse is the above discussed air exchange time constant V/\dot{V} , and if one of the chamber volume or ventilation volume flow is known the other can be determined. Here, with the given chamber volume the volume flow is found to be $0.5605 \text{ m}^3/\text{s}$ with a standard deviation of $0.005 \text{ m}^3/\text{s}$. The volume flow was found to depend on ambient pressure, and this identification should thus be repeated on the day of the evaporation tests.

In addition, if the volume flow of the ventilation is known by measurement, similar tests can be used to validate the overall model. A known amount of helium (or hydrogen) can be released either in one moment as above or repeatedly if equipment allows and the calculus (Eqs. (11), (13) or (15)) using measured values must give the amount released. This was repeatedly checked.

3.3. Evaporation test and accuracy analysis

Real hydrogen system emission tests were conducted with a hydrogen vehicle. The test shown here included a parking phase from 1 to 2523 s, then a test ride up to 3842 s, where another parking phase is monitored up to 7100 s (Fig. 4).

The left plot in Fig. 4 shows the hydrogen concentration measured with a 2 min interval. On the right side the emissions of the car for each time interval are displayed.

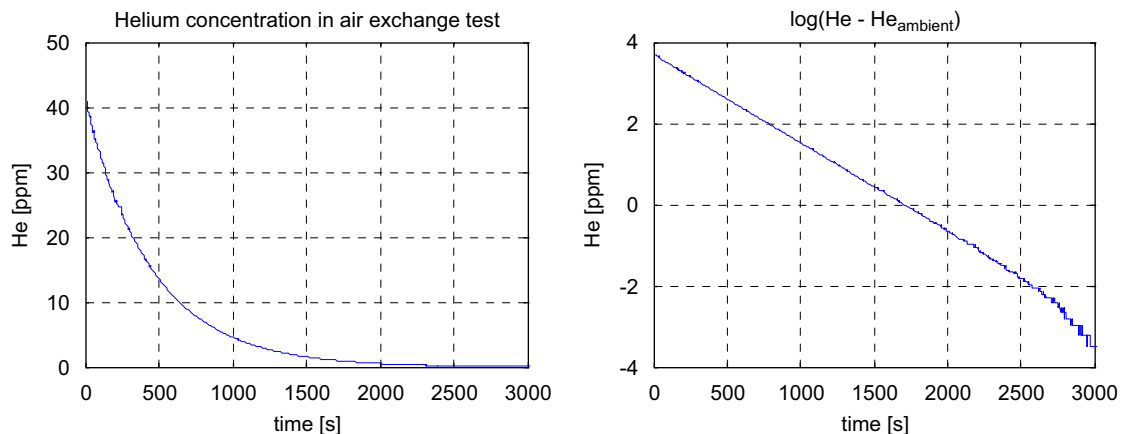


Fig. 3 – Determination of air exchange rate by helium injection experiment.

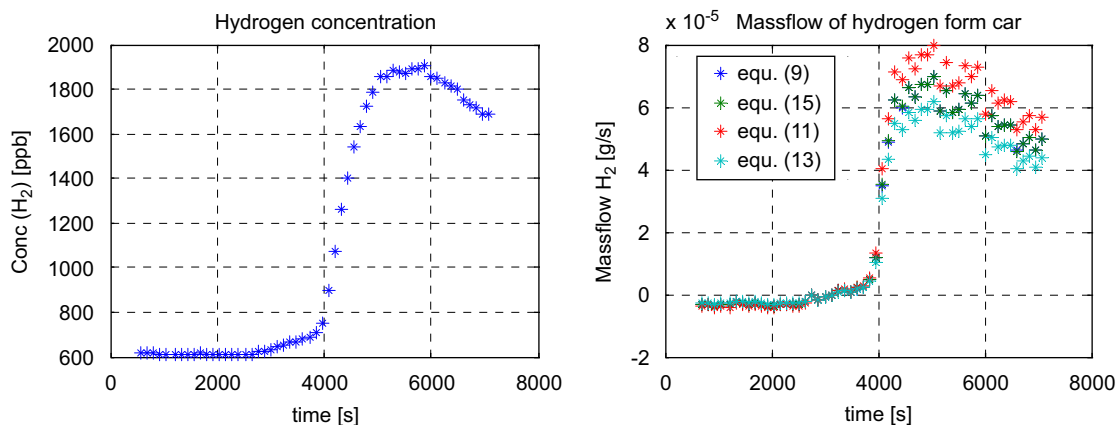


Fig. 4 – Evaporation test: left: chamber concentration, right: calculated emission mass flow. Note: Although the shape of the left and right curve appears similar, the right one is sharper because it includes the derivative of the left curve.

They are calculated applying the different methods and assumptions, i.e. Eqs. (9), (11), (13) and (15).

For the given situation with a chamber volume of 256 m^3 , a ventilation volume flow of $0.5605 \text{ m}^3/\text{s}$ (giving an air exchange time constant of 463 s or 7.72 min) and a sampling rate of 2 min, the accuracy results are as follows: The approximate formula (9) and the accurate formula (15), both assuming that the vehicle emissions are constant over one sampling interval differ less than 0.5% from each other. The values calculated by the worst case equations (11) and (13), assuming short emission peaks at the beginning or end of the sampling intervals, produce errors of 14% and -12% . As can be seen from the overall characteristic of the mass emission curve (Fig. 4, right), however, it is very implausible that the emissions of the vehicles are peak-like and those peaks exactly synchronised with the sampling. Thus, the real accuracy locally, when emissions start or stop, may be as uncertain as -12% to 14% . The overall or aggregated emissions, however (as displayed in Fig. 5), will show a much higher accuracy in all practical cases.

From Figs. 4 and 5 it can be readily seen that this vehicle shows rather small system emissions while running, i.e. 0.0046 g after a 21 min ride (3842 s). Conversely they rise remarkably after system stop. The maximal gas flow reaches $4.32 \text{ mg}/\text{min}$ some 20 min (1200 s) after engine stop and decreases slightly afterwards. Obviously some parts of the hydrogen system leak after system stop until they are exhausted.

Note that all variables such as ventilation flow and ambient concentrations are considered to be constant within each time step. If they vary slowly and their values are measured, this methodology is also applicable with the same accuracy.

3.4. Sensitivity analysis

The sensitivity to measurement errors of this method can be analysed by standard error propagation methods [12]. It shows that random errors in the measurement of the chamber concentration have a considerable impact on the quality of step by step results, caused by building the

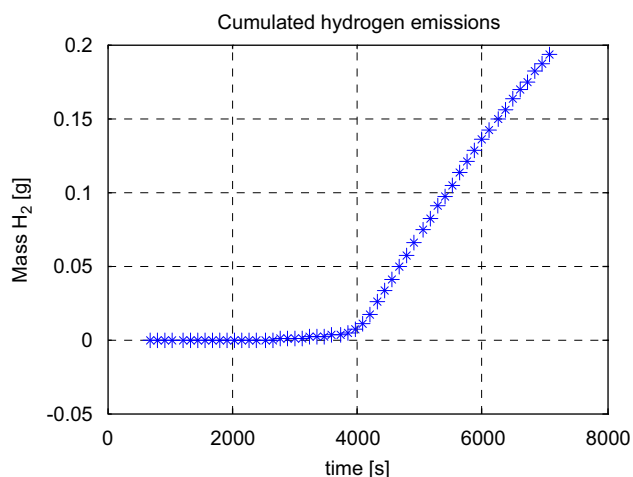


Fig. 5 – Cumulative hydrogen emissions.

difference of two measured values. These errors are, however, compensated when the integral emission is built.

A systematic error of the concentration values, i.e. a bias between the chamber values and the ambient (or inflow) values would result in an incorrect linear trend underlying the integral signal. Such a trend can be detected easily, if the tested vehicle shows phases with assured zero emissions, such as after being stationary overnight. Alternatively, such bias can be reduced by using the same sensor for ambient (intake) and chamber concentration measurements, what is recommended.

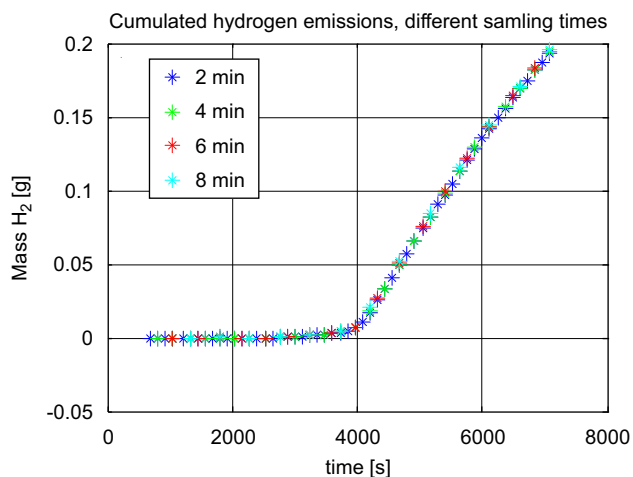
In addition this method is sensitive to the ratio of sampling rate and air exchange rate.

This sensitivity is highlighted by just neglecting intermediate data points in the above example. In this way, the sampling rate can easily be simulated to be a multiple of the original sampling of 2 min. It can be seen in Table 1 that with increased sampling time the range of theoretical uncertainty increases. When the sampling time reaches similar values to the air exchange time constant of 7.72 min, i.e. 6 or 8 min, then the maximal uncertainty rises above 50%, and the values of single steps thus become somewhat

Table 1 – Error between methods as a function of sampling time

Sampling time interval	2 min	4 min	6 min	8 min
Relative error for simplified approach, Eq. (9) (%)	0.4	2.0	4.0	7.0
Relative error for early peak assumption, Eq. (10) (%)	14.2	31.0	51.3	75.6
Relative error for late peak assumption, Eq. (13) (%)	–11.9	–21.9	–30.5	–37.8

Basis for errors is the constant-emitting-source approach (Eq. (15)).

**Fig. 6 – Cumulative hydrogen emissions derived by Eq. (15) with different sampling intervals.**

unreliable. In parallel, the error of the simplified approach of Eq. (9) also rises when sampling time is increased.

This finding coincides with Shannon information theorem postulating that the sampling frequency should be higher than twice of the highest system frequency, thus, here, sampling should be clearly faster than half the air exchange rate. Thus the sampling rate of 2 min fulfils Shannon theorem as the system time constant (air exchange rate) is 7.72 min, what results in the above-mentioned accuracy of –12 to 14%.

Again, since in practice the emissions of the vehicle will not occur in a peak-like manner with multiple peaks synchronised with the measurements sampling, the integral accuracy will be much better than the maximal local errors suggest. This can also be seen in Fig. 6, where the cumulative hydrogen emission curves are almost equal for four different sampling rates. The final error is below 1% for the 8 min sampling compared to the 2 min sampling.

4. Conclusions

A method to measure system emissions for vehicles with gaseous fuels has been introduced. This method is based on

concentration measurements in the test cell and dynamic mass balance calculus. Emissions as small as 2 g per hour are easily detectable.

This method is applicable if the following conditions hold:

- Internal ventilation of test cell is high, so that the chamber concentration can be considered as homogeneously distributed.
- Air exchange rate is at least two times slower than the sampling rate of concentration measurements. Accuracy rises with faster sampling and slower air exchange rate.
- The air exchange rate and the inflow (ambient) concentration of the gas in question must be measured.

The latter is easily feasible if the test cell is air-conditioned by an overpressure system, where all inflow takes place through the A/C duct.

It has been shown by a validating experiment that this method is applicable to practice and gives reliable results and step by step as well as integral quality bounds were given.

Since many exhaust emission laboratories have chassis dynamometers in climate-controlled chambers, this is a cost-effective method to measure system emissions and running losses for the increasing number of vehicles with gaseous fuels such as CNG vehicles and fuel cell or other hydrogen-powered vehicles.

REFERENCES

- [1] CONCAWE, EUCAR, JRC. Well-to-wheel analysis of future automotive fuels and powertrains in the European context, version 2b, May 2006, (<http://ies.jrc.ec.europa.eu/WTW>).
- [2] Romm J. The car and fuel of the future. *Energy Policy* 2006;34(17):2609–14.
- [3] Yeh S, Loughlin DH, Shay C, Gage S. An integrated assessment of the impact of hydrogen economy on transportation, energy use, and air emissions. *Proc IEEE* 2006;94(10):1838–51.
- [4] Ananthackar V, Duffy JJ. Efficiencies of hydrogen storage systems onboard fuel cell vehicles. *Solar Energy* 2005;78(5):687–94.
- [5] Zhang JS, Fisher TS, Ramachandran PV, Gore JP, Mudawar I. A review of heat transfer issues in hydrogen storage technologies. *J Heat Transfer—Trans ASME* 2005;127(12):1391–9.
- [6] Brooks DJ, Baldus SL, Diegel HL, Gorse RA, Sherby RD. Running loss test procedure development. *SAE Technical Paper Ser* 1992;9203(22):209–55.
- [7] Guenther M, DeWaard D, LaPan M, Jensen T, Siegl W, Baldus S, et al. Comparison of vehicle running loss evaporative emissions using point source and enclosure measurement techniques. *General Emissions SAE Special Publications* 1998;1335:131–43.
- [8] Greenwood NN, Earnshaw A, Chemistry of the elements. Butterworth-Heinemann; 2001. p. 56.
- [9] Steinbacher M, Fischer A, Vollmer MK, Buchmann B, Reimann S, Hueglin C. Perennial observations of molecular hydrogen (H_2) at a suburban site in Switzerland. *Atmos Environ* 2007;41:2111–24.
- [10] Novelli PC, Lang PM, Masarie KA, Hurst DF, Myers R, Elkins JW. Molecular hydrogen in the troposphere: global distribution and budget. *J Geophys Res* 1999;104:30427–44.
- [11] Nise NS. Control system engineering. New York: Wiley; 2006.
- [12] Gertsbakh II, Measurement theory for engineers. Berlin: Springer; 2003. p. 87ff.